Microchemical Journal 220 (2026) 116337

Contents lists available at ScienceDirect

Microchemical Journal

journal homepage: www.elsevier.com/locate/microc

Comparative studies of different signal acquisition systems in microfluidic paper-based analytical devices developed for accurate point-of-care analysis

Mafalda G. Pereira [a], Teresa R.S. Brandão [a], António O.S.S. Rangel [a], Raquel B.R. Mesquita [a,*], Víctor Cerdà [b]

[a] Universidade Católica Portuguesa, CBQF – Centro de Biotecnologia e Química Fina – Laboratório Associado, Escola Superior de Biotecnologia, Rua Diogo Botelho 1327, 4169-005 Porto, Portugal
[b] Sciware Sistems/SL, 07193 Bunyola, Spain

ARTICLE INFO

Keywords:
μPAD
Smartphone detection
Accurate quantification
User-friendly analysis

ABSTRACT

The exponential growth of small, on-hand devices/sensors has been aligned with the increasing use of smartphones as detectors. However, smartphone detection may result in high variability of signal acquisition, due to differences in lighting conditions, consequently compromising accurate and reliable quantification. The use of smartphones for qualitative assessment ("yes/no" response) has been widely employed; however, their use in quantitative assessment has been less reported. For point of care (POC) analysis, the use of smartphones as detectors can be an exceptional advantage; however, it is crucial to ensure that the accuracy of the analysis is not compromised. A critical and structured evaluation of image acquisition systems was performed to evaluate the impact on POC biomarkers quantification with microfluidic paper-based devices (μPADs). Different image acquisition systems were tested for a μPAD to properly evaluate the impact of lighting conditions when using a smartphone in a specially designed box. The decrease in intensity counts was about 30% from the scanner to the smartphone, but it did not affect the calculated absorbance. We proved that smartphones can be used as reliable detection systems, providing accurate and precise quantification when appropriate attention is given to exterior lighting conditions. When quantifying iodide and nitrite in a sample, a relative error of 5% was observed for both image-acquiring systems, a scanner and a smartphone.

1. Introduction

In recent years, people have become more self-aware of the impact on health conditions of potential problems arising from the environment and foodstuffs. Consequently, the demand for quick and efficient platforms to attain fast and accurate information about contamination, disease indicators and food composition has increased [1,2]. In this context, there is a growing interest in innovative analytical tools to perform point-of-care (POC) analysis, being user-friendly, rapid, portable and affordable techniques. The idea is that these POC analytical tools do not require trained personnel or expensive equipment, allowing them to obtain a response outside of specialized facilities [3]. Microfluidic paper-based analytical devices (μPADs) play a key role in POC testing as they comply with all the listed characteristics. Paper testing was first reported back in the 1800s, with litmus paper for alkalinity assessment, before the universal indicator for pH determination and has evolved significantly, being extensively used for analytical tests throughout the years [4]. With the advances in imaging tools, the possibility of attaining accurate measurements with paper devices has become a reality. Consequently, μPADs have proven to be useful analytical platforms and an alternative to the conventional microfluidic approaches, due to their high precision and low volumes required [5–7]. In fact, μPADs have been developed targeting important parameters in healthcare, environmental safety, and food quality that can affect the populations' well-being; they can be used in field applications, including in developing countries, where access to conventional procedures is limited [8,9]. The use of paper as a base material for colourimetric determination has important advantages, namely its white colour, availability, functionality, and easy disposal [10]. This way, developing μPADs follows the ASSURED guidelines established by the World Health

* Corresponding author.
E-mail address: rmesquita@ucp.pt (R.B.R. Mesquita).

https://doi.org/10.1016/j.microc.2025.116337
Received 24 December 2024; Received in revised form 11 November 2025; Accepted 24 November 2025
Available online 25 November 2025

Organization involving diagnosis devices, being affordable, sensitive, specific, user-friendly, rapid, robust, equipment-free and deliverable to end-users [11].

There are many fabrication techniques for microfluidic paper devices, such as photolithography, plasma treating, wax printing, plotting, wax dipping, inkjet printing, flexographic printing, laser treatment, stamping and, for three-dimensional (3D), there are also folding and stacking techniques [12]. The 3D structure, attained by folding or stacking paper layers, enables higher efficiency and flexibility in the determination because of enhanced vertical flow within the device [13]. Several detection technologies can be employed for signal acquisition in these devices, such as electrochemistry, electrochemiluminescence, colourimetry, fluorescence and chemiluminescence [14]. Consequently, different detectors can be used, namely, potentiometers, digital cameras, scanners, microscopes, optical fibers spectrometers, and, as a recent trend, smartphones have been gaining popularity [7,15]. The colourimetric determinations have been the privileged choice of detection in μPADs development, as they enable obtaining both semi-quantitative and quantitative results [16]. The detection of the colour product can be attained by image capturing, which makes smartphones an appealing choice. However, the lighting conditions, the distance to the device and the angle at which the image is captured can affect the signal, contributing to increased variability of results [17]. Recently, efforts have been made to manage these types of variations for detection systems, as reported by Phansi et al. [18], by using customized devices for acquiring images and increasing the repeatability of the methods. The simplicity and cost-effective solution represented using smartphones as detectors requires particular attention to lighting and image processing [19,20]. Nevertheless, diagnosis through smartphone detection is becoming easier and much more efficient, especially in a scenario where there are limited resources, being easy to operate, portable and providing real-time analysis [21,22]. Several applications using smartphone detection have been reported from biological analysis, quantification of bacteria, enzymes, pathogens, and many other factors and were summarized in Table 1.

Most of the reported works, using smartphones, account for the potential effect of external lighting in the acquisition of the image [25–31], and most of those even mentioned the need for a specially designed adaptor to minimize that impact [26–29,31]. However, different methods and different determinations make it unclear to assess the real impact on the quantification process.

At the Automation and Miniaturization laboratory of the Centre of Biotechnology and Fine Chemistry (CBQF) of Catholic University of Porto, we have developed an innovative μPAD assembly using just filter paper and laminating plastic pouches. This represents an environmentally friendly approach as there is no need for wax/inkjet/flexographic printing or wax dipping. The μPADs assembled with this technique are based upon a vertical flow approach and can employ the stacking of several filter paper discs, from two to four layers [33,34]. Based on the vertical flow approach, this assembly process enhances the device's versatility by manipulating the number of staked paper discs (and their composition), which can be adjusted for each determination. The developed devices were always based on colourimetric reactions, targeting mainly health indicators [33–35] but also parameters for food quality assessment [36,37]. The detection employed has always been the digital scanner for image acquisition, as it can provide crucial advantages regarding image acquisition, providing a uniform and reproducible imaging of the μPAD [38], which images were treated with free image software (Image J). Nevertheless, as the described devices were only applied using a scanner, there is no evidence that the reported advantages would be lost if another type of detection were used, namely, another form of image acquisition. There are a couple of works by Vaishampayan et al. [39] and Chen et al. [40], that uses smartphone image acquisition combined with a specially designed box. However, in the work of Vaishampayan et al. [39], the aim was to develop the box itself, with no comparison to other acquisition systems, such as scanners or commercial boxes. In the work by Chen et al. [40], not only no other acquisition systems were tested, but also the designed box was to be used with microfluidic chip.

So, in this work, we aimed to evaluate the impact on the acquired signal of using different image acquisition systems, namely a scanner, a webcam, and a smartphone. The broad use of these different acquisition systems fully justifies a structured, comprehensive comparison. For an accurate comparison, previously designed and validated microfluidic devices [37,41] were used with different acquisition systems. In this scenario, images were collected with the different systems and the variability of the intensities was compared. Additionally, several lighting conditions were also tested for the webcam and smartphone image-acquiring system. To attain this, a couple of specially designed boxes with a set of LED lights to control the intensity of the lights were constructed to compare to the other image acquisition systems. The intensity counts of all acquired images were obtained with the free software Image J and using RGB (red, green, and blue) filter.

2. Materials & methods

2.1. Reagents and solutions

All solutions used in this work were prepared with analytical grade chemicals and Milli-Q water, with resistivity >18.2 MΩ/cm (Millipore, USA). The following reagent solutions were prepared according to the description in previously reported works for iodide [37] and for nitrite determination [41].

The 5 M hydrogen peroxide stock solution was prepared by dilution

Table 1
Summary of some previously reported works based on smartphone image acquisition used as detection system in analytical determinations.

Method	Objective	Advantages	Limitations	Reference
Paper-based device	Determination of vancomycin in drugs	Low cost and simple implementation	Slightly higher limit of detection	[23]
Screening system	Latent tuberculosis infection screening	Faster than the traditional method, portable, and accurate	Internet connectivity required	[24]
Chip scale microscope		Low cost, no light source required	Affected by external light changes	[25]
Cytometry platform	Blood analysis	Cost-effective, compact, and accurate	Adaptor needed, high specifications in image selection	[26]
Fluorescence microscope	Pathogenic bacteria identification	Compact, cost-effective	Adaptor needed	[27]
Microscope	Quantification of parasites	Automated, low false-negative rate	Adaptor needed	[28]
Paper-based device	Quantitative fluorescence assays	Inexpensive, sensitive point-of-care assay	Adaptor and specific excitation source needed	[29]
Paper-based device	Glucose sensor	Sensitive, low interference	External lighting not controlled	[30]
Paper-based device	Salmonella quantification	Low-cost, portable, easy-to-use	Adaptor needed	[31]
Real-time loop-mediated isothermal amplification	Pathogen diagnosis	Faster, no false-positive	Heating necessary	[32]

of the commercial solution (d = 1.11, 30 %, Merck). The working peroxide solution was daily prepared by dilution of 10 μL of 5 M hydrogen peroxide stock solution 240 μL of acetic acid 0.8 M. The 3,3′,5,5′-tetramethylbenzidine (TMB) solution was prepared by dissolving 24 mg of TMB (Sigma-Aldrich) in 50 mL of ethanol (96 %, Labchem) and then adding 50 mL of water, resulting in a 1 mM concentration, was stored in a dark bottle and refrigerated. A 0.1 M iodide stock solution (Hanna HI4011–01) was used to prepare two intermediate iodide standard solutions of 5 mM and 0.250 mM. The 0.8 M acetic acid solution was prepared by diluting 4.6 mL of acetic acid (d = 1.05, 100 % glacial, Merck) in 100 mL of water. Then, the pH was adjusted to 3.6 with NaOH 2.5 M, as previously reported [37].

An iodide pharmaceutical tablet (Yodafar 300) containing 300 μg of iodide, according to supplier information, was used as a certified sample. One tablet was weighed (183.8 mg) and crushed in a mortar. Then, 174.4 mg of the crushed tablet was dissolved in 25 mL of water, resulting in an iodide reference solution of 287 μg/L (0.0906 mM).

The Griess reagent was prepared by dissolving approximately 0.4 g of sulfanilamide (Sigma Aldrich) in 2 mL of 5 M orthophosphoric acid and 0.04 g of N-(1-naphthyl)ethylenediamine dihydrochloride (N1NED) (Merck) in water. These two solutions were mixed to a final volume of 20 mL. A 13 mM sodium nitrite (Merck) stock solution was prepared by dissolving approximately 20 mg of the previously dried (overnight at 100 °C) solid in 25 mL of water. A dilution to 2.5 mM was used as an intermediate stock solution to prepare the working standards of nitrite in the range of 5–20 μM, as reported [41].

2.2. Assembly of the microfluidic paper-based devices (μPADs)

The μPADs assembled for this study were prepared with the previously described technique developed in our laboratory, consisting of filter paper discs (hydrophilic zone) aligned within a laminating plastic pouch (hydrophobic zone). The devices are established with 24 reading units in 4 lines and 6 columns arrangement, enabling loading one blank and 5 standards/samples with four replicas each or one blank and 3 standards/samples with six replicas each.

The idea of having several replicas (either 4 or 6) intends to provide accurate and precise results, meaning that image acquisition must not have intrinsic variability. Each reading unit, the hydrophilic detection area, was composed of two stacked paper discs, where the reaction occurred. The filter paper discs were obtained by cutting Whatman filter paper with 9.5 mm diameter discs using a paper puncher (3/8" EK tools). The reading units were separated by the hydrophobic area established using a plastic laminating pouch (75 × 110 × 0.125 mm, Q-Connect). The top sheet of the laminating pouch was perforated with twenty-four 3 mm holes, in the mentioned arrangement of 6 columns × 4 lines, for standard/sample insertion ("Top Layer" in Fig. 1A). The lamination process, performed after the alignment of the stacked paper discs with the sample holes of the plastic laminating pouches (Fig. 1A), is made using a hot laminator (A3-330C High Quality Laminator) to seal the plastic pouch top and bottom layers. The lamination sets the arrangement of 6 columns (C1 to C6 in Fig. 1B) and 4 lines (L1 to L4 in Fig. 1B) of the twenty-four individual reading units (Fig. 1B).

The reading of the device, image acquisition, was made on the bottom layer side (second layer in Fig. 1A) since it corresponds to the colour reagent layer.

The image acquisition of the μPAD was made at different operational moments: i) after preparing the μPAD but before loading the standard or sample, representing a blank (empty) device (Fig. 1B); ii) after loading a single standard in all reading units (ESI Fig. 1); iii) after loading different standards (and/or samples) in different columns (Fig. 1C and D).

2.2.1. Device for iodide determination

The paper sensor for the determination of iodide was previously

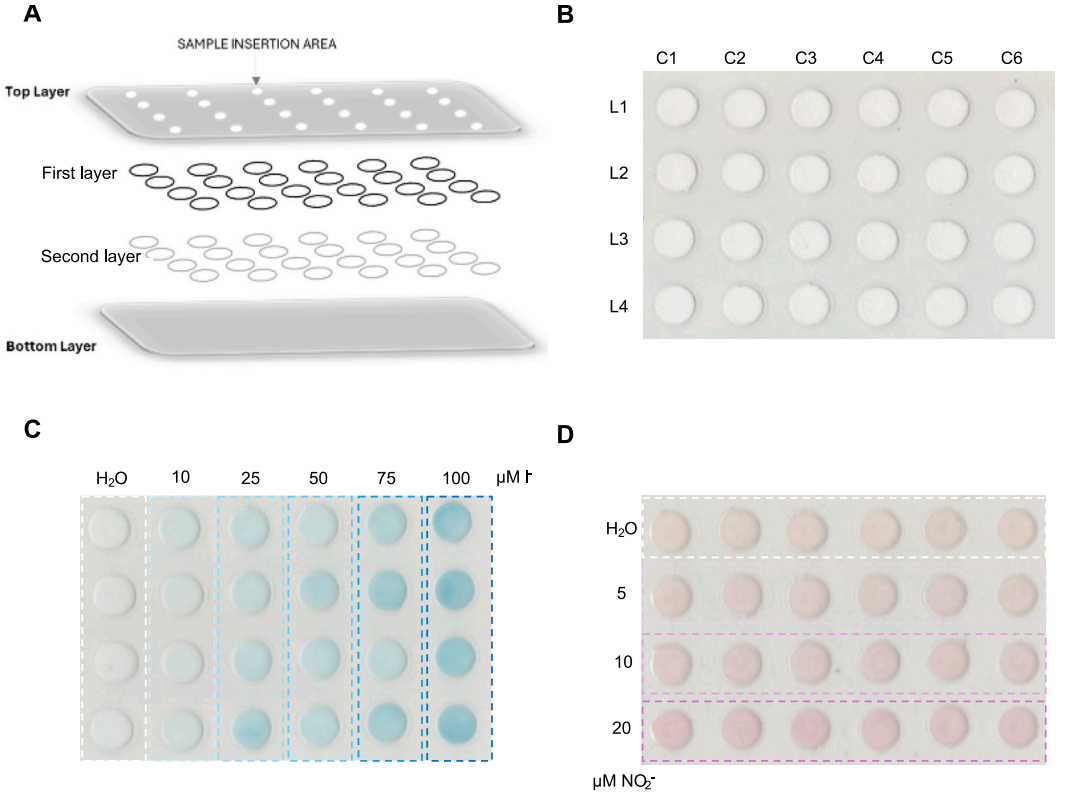

Fig. 1. Microfluidic paper device (μPAD); (A) schematic representation of the alignment; (B) image scan of the device before loading any solution, where L_i represents the lines and C_i the columns of the μPAD; (C) image scan of the iodide determination device after loading the standard solutions, corresponding to a calibration curve; (D) image scan of the nitrite determination device after loading the standard solutions, corresponding to a calibration curve.

developed and validated, by Pereira et al. [37] for the quantification of iodide in dietary supplements. The first layer of discs consisted of Whatman Grade 4 (W4) filter paper loaded with 10 μL of the hydrogen peroxide working solution and set to dry in the oven, at 50 °C for 10 min (first layer in Fig. 1A). The second layer of discs, corresponding to the colour reagent layer, consisted of Whatman Grade 1 (W1) filter paper, loaded with 10 μL of TMB solution and left to air dry at room temperature for 20 min (second layer in Fig. 1A).

2.2.2. Device for nitrite determination

The μPAD employed for nitrite determination had been previously developed and validated by Ferreira et al. [41] for the quantification of nitrite in saliva samples. The first layer consisted of empty discs of Whatman Grade 1 (W1) filter paper (first layer in Fig. 1A). The second layer of discs, corresponding to the colour reagent layer, consisted of Whatman Grade 50 (W50) filter paper, loaded with 10 μL of Griess reagent and set to dry in the oven, at 50 °C for 10 min (second layer in Fig. 1A).

2.3. Image acquisition systems

2.3.1. Digital scanner and photo boxes

As mentioned above, the aim of the developed work was the comparison of the acquisition systems methods, namely, to evaluate the effective use of smartphones for in situ, point-of-care detection method for paper-based analysis. It was performed using a couple of μPADs previously reported, one for iodide determination [37] and one for nitrite determination [41] in which the image acquisition was the Epson Stylus X100 scanner (Fig. 2A). A commercially available box, indicated for photo purposes, the Lightbox Studio XL, Green Stuff World (Fig. 2B) was also used for comparison purposes. This box is partially open, and the image acquisition with the smartphone was taken from the top, where there is a hole for that purpose. As this box is commercially available with specific instructions to be used with a smartphone, it was not used with the webcam.

A couple of boxes were designed with the exact dimensions of the developed μPAD with a hole on top (2.7 cm), for adjusting the webcam/smartphone, and a removable bottom to place the μPAD card (Fig. 2C). The first designed box, a white box, was obtained by resin 3D printing using white resin; the second box, a black box, was an improved version of the white box, as it was painted black on the outside, to minimize interferences from exterior light. Inside, both boxes were white, maintaining a similarity with the commercially available Lightbox Studio XL and the Epson Stylus X100 scanner (also both white inside).

2.3.1.1. LED circuit used in the designed boxes. The designed boxes had two LED strings which were placed on the top part inside the box to guarantee the same lighting conditions inside the box for each of the acquisitions (Fig. 3 A and B). The idea of using LED strips was based on the efficient lighting from the commercially available Lightbox Studio XL, which also used lateral LED strips.

Various devices were tested to regulate the intensity of LEDs, whether voltage or intensity regulators. Finally, the voltage regulator was selected, the electronic diagram of which is represented in Fig. 3C, and which is based on the LM317 surface-mount chip. The design of the schematic circuit and the board was carried out using the Eagle program. Both schemes are represented in Fig. 3, along with a photograph of the final device (Fig. 3 D and E).

2.3.2. Image capturing – smartphone and webcam

The images were captured using a smartphone camera (iPhone 13) and a webcam (Microsoft Lifecam Cinema for Business) and were compared to the images obtained with the scanner. The settings for the iPhone 13 camera were: autofocusing feature, 12 MP wide-angle sensor, aperture: f/1.6, focal length: 26 mm equivalent, automatic shutter speed range: 1/8000–1 s, and pixel size: 1.7 μm. For the webcam, the settings were: CMOS sensor, up to 5 MP interpolated still image resolution at 640 × 480, wide-angle lens with 73° field of view, autofocus and digital zoom when using the YouCam 365 software.

2.4. Image processing

The acquired images of the μPAD were obtained using different acquisition methods (Microsoft Corporation Scanner software, Cyberlink YouCam, AMCap, etc.) and analysed by the free image processing software, ImageJ. The intensity measurements were obtained for each paper disc unit, using RGB (Red, Green, Blue) filters. The selected filters were the red filter for the iodide determination, corresponding to the complementary colour of the resulting light blue coloured product, and green filter for the nitrite determination, corresponding to the complementary colour of the resulting pink coloured product (ESI Fig. 2). The comparison between acquisition methods was made by comparing the average of the intensities of the reading units in each column and line in the device (Fig. 1B).

2.4.1. Data analysis

For two of the image acquisition methods, namely the scanner and the smartphone with the designed black box, an ANOVA was performed, aiming at detecting differences in the intensity between lines and columns of the μPAD. Duncan's test was subsequently used for means comparison between different groups of intensities. Normality and homoscedasticity of data were assessed by using Kolmogorov-Smirnov and Levene's tests, respectively. The significance level was assumed to be 1% in all cases.

3. Results and discussion

3.1. Scanner vs smartphone photo

For the first study, the use of a scanner to capture the μPAD image for

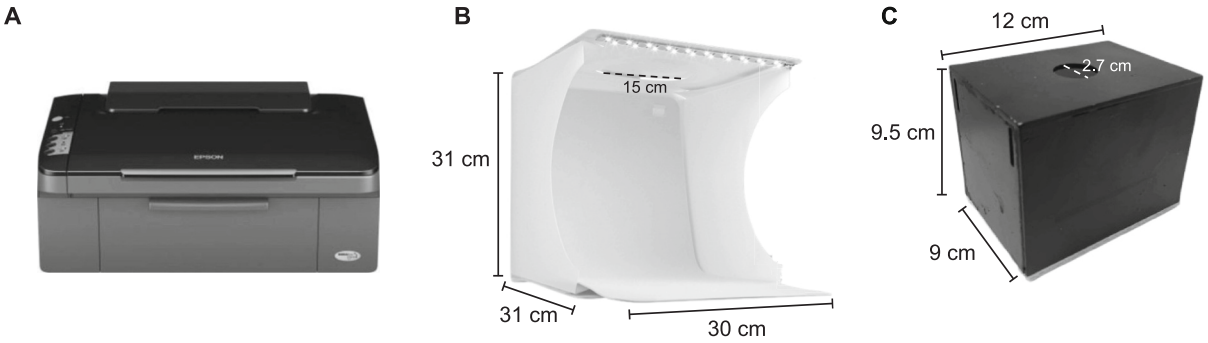

Fig. 2. Different acquisition methods: (A) Epson Scanner; (B) Lightbox Studio XL for smartphone photo; (C) specially designed box for smartphone and webcam use.

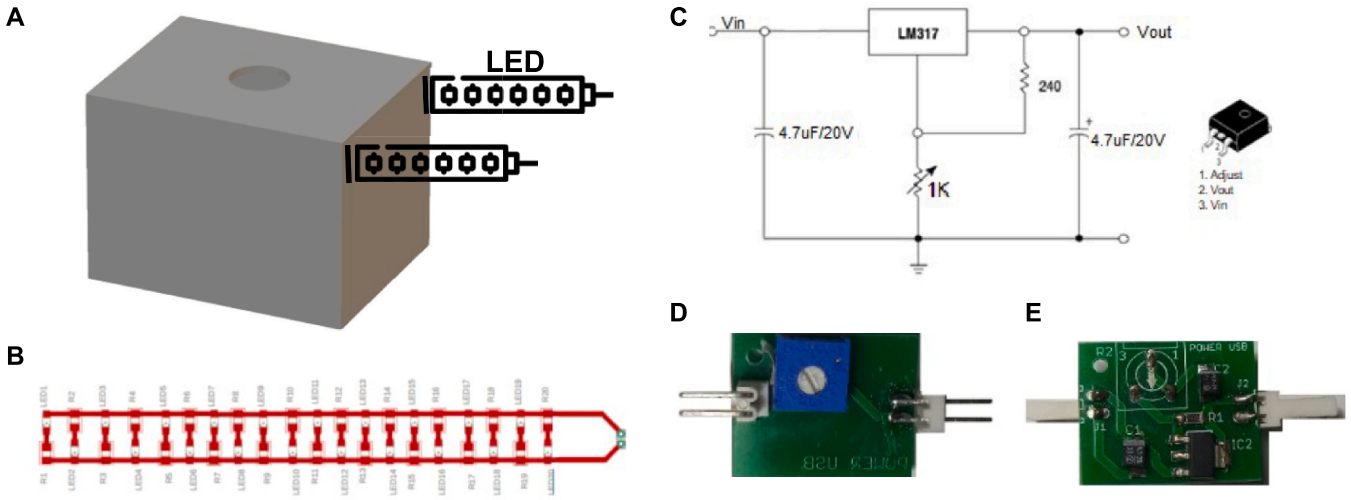

Fig. 3. (A) A schematic representation of the LED placement in the stereolithographic printed box; (B) Eagle-designed schematic electronic circuit for the LED strips to be connected to the power source; (C) Schematic diagram of the voltage-regulated power supply; (D) Top and (E) Bottom photography of the power supply device.

processing in the ImageJ software was set as a reference acquisition system. Then, the alternative methods to be tested for image acquisition were compared to the scanner-acquired images. This study used a freshly prepared, but empty μPAD (Fig. 1B), so the same intensity counts were expected for all #24 reading units, independently of the column/line arrangement. The comparison was between the scanner, the Lightbox Studio XL used with a smartphone and the designed white box used with both the webcam and smartphone (Fig. 4).

The most notable difference is that the image acquired with the scanner resulted in higher intensity values than the smartphone (in both boxes) and the webcam, where a decrease of about 30% in intensity counts was observed. However, the absolute intensity is not a problem itself as the accurate quantification is attained by a logarithmic calculation of intensities into pseudo-absorbance. When comparing the intensity averages from lines and columns, it was possible to observe higher variability with both boxes (Lightbox Studio XL and the white box) than with the scanner. A potential explanation for the variability could be that external lighting conditions had interfered with the image reading, as, with the scanner, the lighting conditions are not susceptible to external variation.

Additionally, although both boxes had LED lights incorporated, they were different as the Lightbox Studio had one side open and the designed white box was fully closed (Fig. 2 B and C) so it was expected to have less external lighting impact than the Lightbox Studio.

However, that was not the case, and despite being fully closed, the designed white box proved to have a higher variability (especially when used with the smartphone) and wider variation compared to the average intensity calculated (Fig. 4 horizontal orange line). This could be explained by the presence of the internal LED lighting of the Lightbox Studio together with the opacity of the material which helped to minimize the influence of the external lighting (grey bars compared to the horizontal grey line in Fig. 4). Even though the commercially available Lightbox Studio presented an acceptable variation, its overall size and the fact that is open on one side, impaired its effective field application.

3.2. *Evaluation of external light impact*

The source of the variability in the intensity values obtained with the

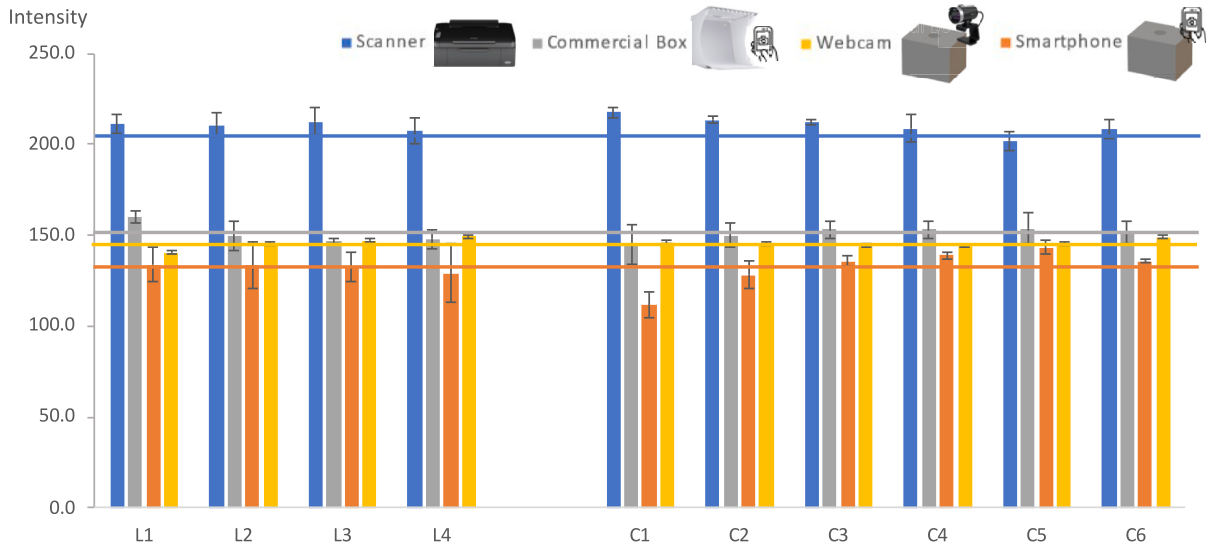

Fig. 4. Comparison of average intensity values of the μPAD lines and columns of reading units for different image acquisition methods; the horizontal lines represent the overall intensity value average for the entire device measure for each method; the error bars represent the standard deviation.

designed white box was important to assess. So, different lighting conditions were tested (ESI Fig. 3), and the average intensity values of the μPAD reading units arranged in lines and columns were compared. Images were acquired with LED lighting inside the white box and no other external lights (ESI Fig. 3A), with a ceiling halogen lamp on top of the box (ESI Fig. 3B) and with a desk lamp directed at the white box (ESI Fig. 3C). For this study, two acquisition systems were used, smartphone and webcam placed at the top hole of the designed box, to evaluate if the obtained intensity counts variability was due to the difference in exterior lighting conditions or the image acquisition device (Fig. 5). Considering the differences in the exposure conditions of the webcam and smartphone, both were used in this external lighting study. The external lighting was kept the same for both systems.

Using the smartphone, all different lighting conditions presented high variability of intensity values, in particular the directed light to the box (Fig. 5A, grey bars). This direct light into the box also resulted in high intensity count values, with the average intensity of the complete device higher (grey line in Fig. 5A).

The top light and LED light intensity counts values resulted in similar intensity values and average but a lower intensity average than the direct lamp light (orange and blue horizontal lines in Fig. 5A). Furthermore, the variability of the calculated intensities also increased (standard deviation error bars in Fig. 5A). A potential explanation could be the fact that the box was white and consequently transparent enabling the exterior light to go through but not evenly distributed to the μPAD.

The results obtained with this study enable us to conclude that using different external lighting has a direct impact on the intensity counts variability and, consequently, on the acquired signal.

The results using the webcam (Fig. 5B) support the previous conclusion but with less pronounced differences. In fact, when using the webcam, the intensities count obtained with the LED lighting were lower (blue bars in Fig. 5B) than the intensities counts obtained with top ceiling light and direct lamp (orange and grey horizontal lines in Fig. 5B).

Based count results observed, improvements were made to the box, aiming to solve the external light impact. As the highest impact had been observed when using the smartphone, the next studies only involved a smartphone as an image acquisition device. The aim was to make sure the smartphone could provide an easier and more feasible reading device for quantification.

3.3. Reducing exterior lighting interference

To minimize the impact of exterior lighting conditions, an improvement was performed on the designed box, maintaining the same dimensions but painting it black on the outside (Fig. 2C), which was named the black box.

With this new, improved box, no image could be captured without the LED inside the box, assuring that no light was passing through the black box. So, a different study was conducted, using the LED light strips inside the box (on the top sides of the box, as shown in Fig. 3A).

For this study, two devices were assembled as described in section 2.2, one was loaded with deionized water (simulating a blank signal, Fig. 1B), and one was loaded with a 100 μM iodide standard solution (ESI Fig. 1). Both devices were given the 25-min reaction time, as previously reported [37] before making the image acquisition for intensity readings. As each μPAD was entirely loaded with the same solution, the same intensity counts were expected for all #24 reading units, independently of the column line arrangement (ESI Fig. 4).

Image acquisition was made using the scanner and the smartphone, with the black box equipped with LED lights (ESI Fig. 4). As expected, the average intensity with the iodide standard was lower than the average intensity for the blank, and it was the same for both acquisition systems (Table 2).

For the μPAD loaded with the iodide standard, both the scanner and black box with smartphone showed no significant differences from the average values for each column and line of the complete device (dark

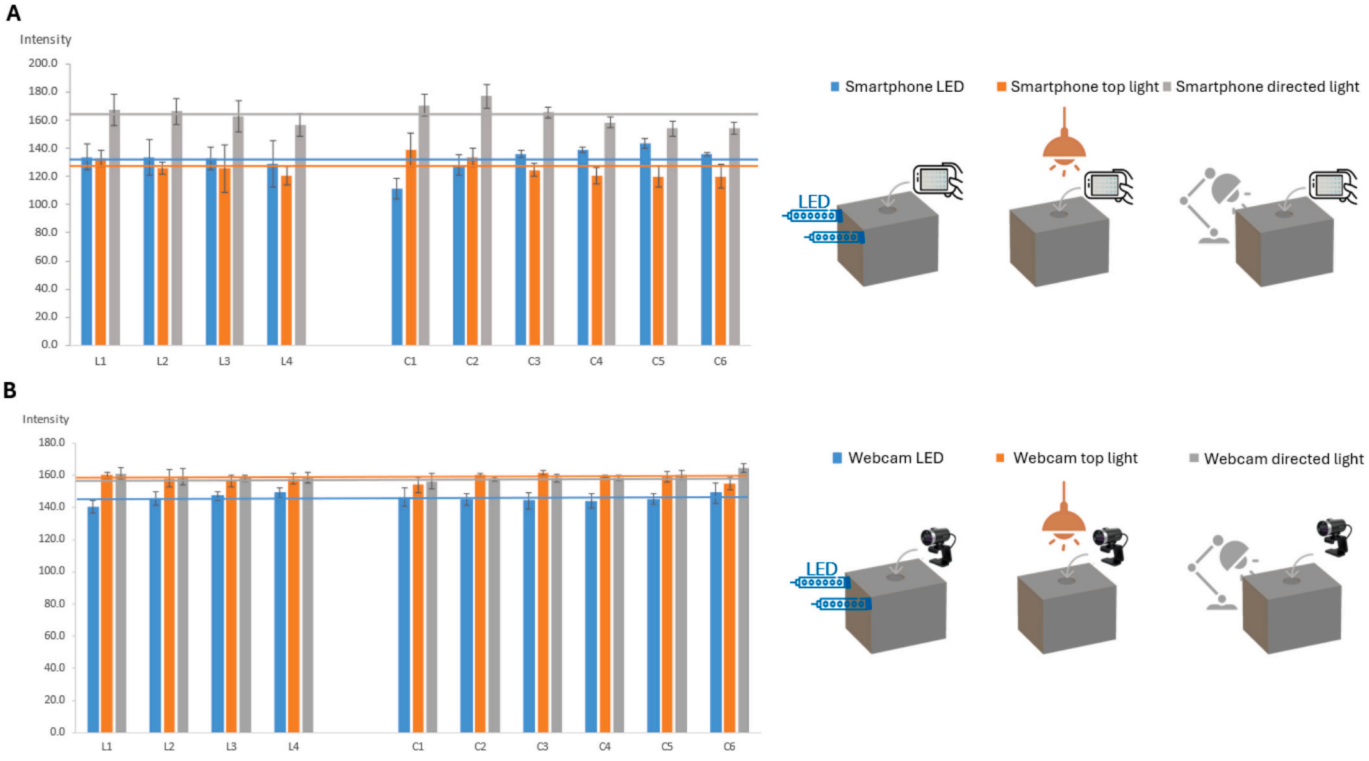

Fig. 5. Different acquisition methods and comparison of readings with the designed white box; (A) comparison of mean intensity values of each line and column of the μPAD for the different lighting conditions, using a smartphone; (B) comparison of mean intensity values of each line and column of the μPAD for the different lighting conditions, using a webcam; the error bars represent the standard deviation.

Table 2
Comparison of the average intensity values obtained with the scanner ($I_{scanner}$) and the black box with smartphone ($I_{smartphone}$) image acquisition; SD, standard deviation.

Loaded Solution	μPAD card	$I_{scanner} \pm SD$	$I_{smartphone} \pm SD$
100 μM iodide solution	Lines L_1-L_4 (#4)	193 ± 1	155 ± 2
	Columns C_1-C_6 (#6)	193 ± 2	155 ± 3
	Entire card	193 ± 1	155 ± 2
Milli-Q water	Lines L_1-L_4 (#4)	206 ± 1	166 ± 1
	Columns C_1-C_6 (#6)	206 ± 3	166 ± 7
	Entire card	206 ± 2	166 ± 5

and light blue bars in ESI Fig. 4). For the blank μPAD, some variations in the average intensity between device columns were observed with both image acquisition systems (dark and light green bars in ESI Fig. 4). Nevertheless, this proved that there were no differences between the two image acquisition systems (Table 2) and the improved black box effectively solved the external light impact.

To further validate this conclusion, a statistical analysis was performed between columns and between the lines for both acquisition systems (scanner and smartphone). No significant differences were found between lines of the μPAD, so no further analysis was detailed. Targeting the intensities of the columns, different observations were made (ESI Fig. 5).

For the device loaded with the 100 μM iodide standard, no differences were found between columns with both the scanner and smartphone (ESI Fig. 5). However, for the device loaded with deionized water, differences were found in both acquisitions. With the smartphone images, the mean intensity increased along the columns (C1 to C6 in Fig. 1B), in which the means from C1 are different from C2 and C3 and different from C4, C5 and C6, dividing themselves into three different groups (ESI Fig. 5). In this way, it was possible to conclude that these results are statistically different ($p = 0.003$). As for the scanner, it was possible to observe that the columns C1, C2 and C3 were different from C6 (ESI Fig. 5), so it was possible to conclude that they were statistically different ($p < 0.001$). Nevertheless, given that in both acquisitions for the blank μPAD there were significant differences, there is no evidence to suggest that the smartphone acquisition is better or worse than the scanner, a conclusion that also corresponds to the device where the standard solution was inserted.

3.4. Absorbance measurements

For quantification purposes, the intensity values were converted into pseudo-absorbance, using the formula $A = \log (I_0/I)$, where A is the calculated absorbance value, I is the intensity values obtained from loading with the standard/sample, and I_0 is the average of intensity values obtained from loading with waters (intensity of the blank). In this study, the absorbance of the #24 reading units of the μPAD loaded with iodide standard (ESI Fig. 1) was calculated using the average of the intensities of the μPAD loaded deionized water (Fig. 1B), as the average of the blank signal. Then, the average of the reading units of the columns and lines arrangement and the average of the entire device were calculated, and a comparison was made between both acquisition systems (Table 3).

The absorbance values calculated with the intensities obtained from the scanner image ($A_{scanner}$) were compared to the corresponding absorbance values calculated with the intensities obtained from the black box/smartphone image ($A_{smartphone}$) by the relative error (RE) calculation: $\%RE = ((A_{smartphone} - A_{scanner})/ A_{scanner}) \times 100$. The calculated absorbances were numerically identical within each image acquisition system and very similar between both systems, with a relative error < 5%.

Table 3
Comparison of calculated absorbance from the intensity values obtained with the scanner ($A_{scanner}$) and black box with smartphone ($A_{smartphone}$) image acquisition; SD, standard deviation; RE, relative error.

μPAD card	$A_{scanner} \pm SD$	$A_{smartphone} \pm SD$	RE
Lines L_1-L_4 (#4)	0.028 ± 0.002	0.029 ± 0.005	5%
Columns C_1-C_6 (#6)	0.028 ± 0.003	0.029 ± 0.006	4%
Entire μPAD card	0.028 ± 0.003	0.029 ± 0.006	4%

3.4.1. Analyte quantification – Iodide and nitrite determination

To evaluate the impact of the smartphone acquisition image in an analytical procedure for quantification, the two devices were compared, employing different coloured reactions and consequently using different RGB filters (ESI Fig. 6). As mentioned, these devices have been previously developed and validated for the determination of iodide [37] and nitrite [41]. As such, an iodide calibration curve and a nitrite calibration curve were established, comparing the smartphone image with the one from the scanner. Two μPADs were prepared, one loading #5 iodide standard solutions (with #4 replicas each), ranging from 10 to 100 μM (Fig. 1C), and another loading #3 nitrite standard solutions (with #6 replicas each), ranging from 5 to 20 μM (Fig. 1D), establishing calibration curves in both (ESI Fig. 6). These calibration curves enabled the determination of iodide and nitrite concentration to be determined by interpolation of the absorbance value of the tested samples. For the sample analysis, additional μPADs were prepared, one loading the pharmaceutical tablet solution, as an iodide sample, and another loading a river water sample for nitrite determination (Table 4).

Both acquisition systems were used as detection systems for the prepared μPADs, and the results were summarized (Table 4). The concentration values of each analyte in each tested sample were obtained based on the calculated absorbance ($[Analyte]_{reported\ value}$) by the relative error (RE) calculation: $\%RE = (([Analyte]_{\mu PAD\ obtained\ value}) - ([Analyte]_{reported\ value}))/[Analyte]_{reported\ value} \times 100$.

The established calibration curves (ESI Fig. 7) showed no significant differences between both acquisition methods (relative error between the slopes <9%). The iodide concentration value obtained for the pharmaceutical tablet sample with the different image acquisition systems was not significantly different from the reference value (relative errors <5%).

In fact, the iodide concentration obtained from the calibration curve (ESI Fig. 7 A) obtained with the scanner was almost the same as the one obtained from the smartphone with the black box (relative error < 1%). The relative error between the average iodide sample concentration of the replicas (#4) in lines and columns was 2% for the scanner and 1% for the smartphone with the black box, respectively.

Table 4
Comparison of the calibration curve values obtained from the scanner and black box with smartphone image acquisition; SD, standard deviation; RE, relative error.

Analyte	Acquisition system	Equation of the calibration curve A = slope × [Analyte] (mM) + intercept	[Analyte] $_{\mu PAD\ obtained\ value} \pm SD$ (mM)	Reported value	RE
Iodide	Scanner	$A = 0.925 \times [I^-] - 0.011$	0.0945 ± 0.002	$[I^-]$ = 0.0906 mM	4%
	Smartphone (black box)	$A = 1.01 \times [I^-] - 0.005$	0.0969 ± 0.005		5%
Nitrite	Scanner	$A = 1.58 \times [NO_2^-] - 0.0007$	0.0040 ± 0.002	$[NO_2^-]$ = 0.179 mg/L (0.00389 mM)	3%
	Smartphone (black box)	$A = 1.53 \times [NO_2^-] - 0.0002$	0.0040 ± 0.003		3%

The nitrite calibration curve (ESI Fig. 7B) also proved to be similar in both acquisition systems, as the slope obtained presented a relative error of −3% when comparing the scanner with the smartphone image. As for the sample validation, it also became possible to state that no differences were found between both image acquisition methods, since the nitrite levels found in the sample were the same for both the scanner and the smartphone.

4. Conclusions

In this work, different image acquisition systems, namely scanner and smartphone, were compared in a structured method using previously developed microfluidic paper-based analytical devices (μPADs) for iodide and nitrite determination [37,41]. These μPADs were assembled with the technique developed in our laboratory, consisting of using filter paper discs aligned (hydrophilic zone) in a plastic laminating pouch (hydrophobic zone) and based on the vertical flow approach. In our previously reported methods [33,35–37] the image acquisition was made using a scanner to avoid light potential interference issues, and, in this study, it was set as a reference. However, the μPAD off-laboratory use is a key feature for point-of-care (POC), so smartphones have been favoured as detectors since they provide an easier "on-hand" approach. In this context, different approaches have been reported on several image acquisition systems, such as optical platforms adapted to restrict lighting conditions so as not to affect the image [42], using only the phone camera and flashlight [30], using the phone camera and exterior lighting conditions [25] and using the smartphone for both image acquisition and treatment [23]. Nevertheless, in those reports, no proper comparison studies were carried out. So, it became pertinent to evaluate the impact of lighting conditions and different image acquisition systems on the quantification process, with a structured comparison to ensure accurate and robust results.

The results proved that the scanner enabled a higher intensity counts and a higher uniformity in the images acquired than the smartphone if there is no external light conditions are accounted for. It showed that, when using a smartphone, external light conditions cause variations in the acquired signal.

To minimize these effects, a closed and opaque box should be employed for smartphone image acquisition. After evaluating the impact in the intensity counts, further signal processing was also assessed by calculating the absorbance, establishing calibration curves and carrying out analytical quantification, which made possible to prove that there was no difference between the smartphone-acquired images compared to the scanner.

In the end, it was proven that a more convenient and portable image acquisition system, namely a smartphone, can be used in a scenario of limited resources using μPADs analysis, as it still provides an accurate quantification. However, it was also proven that exterior lighting conditions do impact image acquisition and the following image processing. The μPADs, with either of these acquisition systems, present the important advantage of being potentially used by individuals without specialized training, suitable for home use, combining a user-friendly approach with affordability and accessibility.

CRediT authorship contribution statement

Mafalda G. Pereira: Writing – original draft, Visualization, Validation, Methodology, Investigation, Formal analysis. **Teresa R.S. Brandão:** Writing – original draft, Methodology, Formal analysis. **António O.S.S. Rangel:** Writing – review & editing, Project administration, Funding acquisition. **Raquel B.R. Mesquita:** Writing – review & editing, Validation, Supervision, Methodology, Investigation, Formal analysis, Conceptualization. **Víctor Cerdà:** Writing – original draft, Resources, Methodology, Funding acquisition, Conceptualization.

Declaration of competing interest

The authors declare that they have no known competing financial interests or personal relationships that could have appeared to influence the work reported in this paper.

Acknowledgement

R.B.R. Mesquita thanks FCT—Fundação para a Ciência e a Tecnologia for the 2022.00962.CEECIND (https://doi.org/10.54499/2022.00962.CEECIND/CP1745/CT0006) and T.R.S. Brandão thanks FCT for the CEECINST/00070/2021/CP1778/CT0010 (https://doi.org/10.54499/2022.00962.CEECIND/CP1745/CT0006). This work was supported by the project COMPETE2030-FEDER-00824900, op. 16,961, supported by FEDER fund within the thematic program Inovation and Digital transition (COMPETE 2030) trough FCT and by National Funds from FCT through project UIDB/50016/2020.

Appendix A. Supplementary data

Supplementary data to this article can be found online at https://doi.org/10.1016/j.microc.2025.116337.

Data availability

No data was used for the research described in the article.

References

[1] C.M. Wang, C.Y. Chen, W.S. Liao, Enclosed paper-based analytical devices: concept, variety, and outlook, Anal. Chim. Acta 1144 (2021) 158–174, https://doi.org/10.1016/j.aca.2020.10.007.
[2] Z. Yao, P. Coatsworth, X. Shi, J. Zhi, L. Hu, R. Yan, F. Güder, H.D. Yu, Paper-based sensors for diagnostics, human activity monitoring, food safety and environmental detection, Sens. Diagn. 1 (2022) 312–342, https://doi.org/10.1039/d2sd00017b.
[3] S.K. Yadav, D. Verma, U. Yadav, A. Kalkal, N. Priyadarshini, A. Kumar, K. Mahato, Point-of-care devices for viral detection: COVID-19 pandemic and beyond, Micromachines (Basel) 14 (2023), https://doi.org/10.3390/mi14091744.
[4] D.M. Cate, J.A. Adkins, J. Mettakoonpitak, C.S. Henry, Recent developments in paper-based microfluidic devices, Anal. Chem. 87 (2015) 19–41, https://doi.org/10.1021/ac503968p.
[5] R. Kumari, A. Singh, U.P. Azad, P. Chandra, Insights into the fabrication and electrochemical aspects of paper microfluidics-based biosensor module, Biosensors 13 (2023), https://doi.org/10.3390/bios13090891.
[6] A.W. Martinez, S.T. Phillips, M.J. Butte, G.M. Whitesides, Patterned paper as a platform for inexpensive, low-volume, portable bioassays, Angew. Chemie – Int. Ed. 46 (2007) 1318–1320, https://doi.org/10.1002/anie.200603817.
[7] N. Okutan Arslan, L. Trabzon, Evaluation of food μPADs with the new tech perspectives and future prospects, EFood 4 (2023), https://doi.org/10.1002/efd2.116.
[8] A.K. Yetisen, M.S. Akram, C.R. Lowe, Paper-based microfluidic point-of-care diagnostic devices, Lab Chip 13 (2013) 2210–2251, https://doi.org/10.1039/c3lc50169h.
[9] B. Selvakumar, A. Kathiravan, Sensory materials for microfluidic paper based analytical devices – a review, Talanta 235 (2021), https://doi.org/10.1016/j.talanta.2021.122733.
[10] R. Álvarez-DIduk, J. Orozco, A. Merkoçi, Paper strip-embedded graphene quantum dots: a screening device with a smartphone readout, Sci. Rep. 7 (2017), https://doi.org/10.1038/s41598-017-01134-3.
[11] A.W. Martinez, S.T. Phillips, G.M. Whitesides, E. Carrilho, Diagnostics for the developing world: microfluidic paper-based analytical devices, Anal. Chem. 82 (2010) 3–10, https://doi.org/10.1021/ac9013989.
[12] T. Ozer, C. Mcmahon, C.S. Henry, Advances in paper-based analytical devices, Annu. Rev. Anal. Chem. (2020), https://doi.org/10.1146/annurev-anchem-061318.
[13] T. Chu, J. Chu, B. Gao, B. He, Modern evolution of paper-based analytical devices for wearable use: from disorder to order, Analyst 145 (2020) 5388–5399, https://doi.org/10.1039/d0an00994f.
[14] Y. Hou, C.C. Lv, Y.L. Guo, X.H. Ma, W. Liu, Y. Jin, B.X. Li, M. Yang, S.Y. Yao, Recent advances and applications in paper-based devices for point-of-care testing, J. Anal. Test. 6 (2022) 247–273, https://doi.org/10.1007/s41664-021-00204-w.
[15] M. Rezazadeh, S. Seidi, M. Lid, S. Pedersen-Bjergaard, Y. Yamini, The modern role of smartphones in analytical chemistry, TrAC – Trends Anal. Chem. 118 (2019) 548–555, https://doi.org/10.1016/j.trac.2019.06.019.
[16] Y. Tao, H. Shen, K. Deng, H. Zhang, C. Yang, Microfluidic devices with simplified signal readout, Sens. Actuat. B Chem. 339 (2021), https://doi.org/10.1016/j.snb.2021.129730.

[17] G.G. Morbioli, T. Mazzu-Nascimento, A.M. Stockton, E. Carrilho, Technical aspects and challenges of colorimetric detection with microfluidic paper-based analytical devices (μPADs) – a review, Anal. Chim. Acta 970 (2017) 1–22, https://doi.org/10.1016/j.aca.2017.03.037.
[18] P. Phansi, S. Janthama, V. Cerdà, D. Nacapricha, Determination of phosphorus in water and chemical fertilizer samples using a simple drawing microfluidic paper-based analytical device, Anal. Sci. 38 (2022) 1323–1332, https://doi.org/10.1007/s44211-022-00162-y.
[19] K.E. McCracken, J.Y. Yoon, Recent approaches for optical smartphone sensing in resource-limited settings: a brief review, Anal. Methods 8 (2016) 6591–6601, https://doi.org/10.1039/c6ay01575a.
[20] N. Alizadeh, A. Salimi, R. Hallaj, Mimicking peroxidase-like activity of Co3O4-CeO2 nanosheets integrated paper-based analytical devices for detection of glucose with smartphone, Sens. Actuat. B Chem. 288 (2019) 44–52, https://doi.org/10.1016/j.snb.2019.01.068.
[21] K. Yang, H. Peretz-Soroka, Y. Liu, F. Lin, Novel developments in mobile sensing based on the integration of microfluidic devices and smartphones, Lab Chip 16 (2016) 943–958, https://doi.org/10.1039/c5lc01524c.
[22] L. Hárendarčíková, J. Petr, Smartphones & microfluidics: marriage for the future, Electrophoresis 39 (2018) 1319–1328, https://doi.org/10.1002/elps.201700389.
[23] K. Mermer, J. Paluch, J. Kozak, Smartphone-based digital image colorimetry for the determination of vancomycin in drugs, Monatsh. Chem. (2022), https://doi.org/10.1007/s00706-022-02964-2.
[24] L. Li, Z. Liu, H. Zhang, W. Yue, C.W. Li, C. Yi, A point-of-need enzyme linked aptamer assay for mycobacterium tuberculosis detection using a smartphone, Sens. Actuat. B Chem. 254 (2018) 337–346, https://doi.org/10.1016/j.snb.2017.07.074.
[25] S.A. Lee, C. Yang, A smartphone-based chip-scale microscope using ambient illumination, Lab Chip 14 (2014) 3056–3063, https://doi.org/10.1039/c4lc00523f.
[26] H. Zhu, I. Sencan, J. Wong, S. Dimitrov, D. Tseng, K. Nagashima, A. Ozcan, Cost-effective and rapid blood analysis on a cell-phone, Lab Chip 13 (2013) 1282–1288, https://doi.org/10.1039/c3lc41408f.
[27] V. Müller, J.M. Sousa, H. Ceylan Koydemir, M. Veli, D. Tseng, L. Cerqueira, A. Ozcan, N.F. Azevedo, F. Westerlund, Identification of pathogenic bacteria in complex samples using a smartphone based fluorescence microscope, RSC Adv. 8 (2018) 36493–36502, https://doi.org/10.1039/c8ra06473c.
[28] M.V. D'ambrosio, M. Bakalar, S. Bennuru, C. Reber, A. Skandarajah, L. Nilsson, N. Switz, J. Kamgno, S. Pion, M. Boussinesq, T.B. Nutman, D.A. Fletcher, Point-of-care quantification of blood-borne filarial parasites with a mobile phone microscope, Sci. Transl. Med. 7 (2015), https://doi.org/10.1126/scitranslmed.aaa3480.
[29] N.K. Thom, G.G. Lewis, K. Yeung, S.T. Phillips, Quantitative fluorescence assays using a self-powered paper-based microfluidic device and a camera-equipped cellular phone, RSC Adv. 4 (2014) 1334, https://doi.org/10.1039/c3ra44717k.
[30] A. Soni, S.K. Jha, Smartphone based non-invasive salivary glucose biosensor, Anal. Chim. Acta 996 (2017) 54–63, https://doi.org/10.1016/j.aca.2017.10.003.
[31] T.S. Park, W. Li, K.E. McCracken, J.Y. Yoon, Smartphone quantifies Salmonella from paper microfluidics, Lab Chip 13 (2013) 4832, https://doi.org/10.1039/c3lc50976a.
[32] L. Barnes, D.M. Heithoff, S.P. Mahan, G.N. Fox, A. Zambrano, J. Choe, L. N. Fitzgibbons, J.D. Marth, J.C. Fried, H.T. Soh, M.J. Mahan, Smartphone-based pathogen diagnosis in urinary sepsis patients, EBioMedicine 36 (2018) 73–82, https://doi.org/10.1016/j.ebiom.2018.09.001.
[33] J.I.S. Aguiar, A.O.S.S. Rangel, R.B.R. Mesquita, Salivary calcium determination with a specially developed microfluidic paper-based device for point-of-care analysis, Talanta Open 8 (2023), https://doi.org/10.1016/j.talo.2023.100254.
[34] F.T.S.M. Ferreira, R.B.R. Mesquita, A.O.S.S. Rangel, On-hand tool for ammonium and urea determination in saliva to monitor chronic kidney disease – design of a couple of microfluidic paper-based devices, Microchem. J. 193 (2023), https://doi.org/10.1016/j.microc.2023.109102.
[35] M.M.P. Melo, A. Machado, A.O.S.S. Rangel, R.B.R. Mesquita, Disposable microfluidic paper-based device for on-site quantification of urinary creatinine, Chemosensors 11 (2023), https://doi.org/10.3390/chemosensors11070368.
[36] R.B.R. Mesquita, C. Klima, H. Martínez-Pérez-Cejuela, A.R. Monforte, A.C. S. Ferreira, A.O.S.S. Rangel, Targeting iron speciation in wines: design of a microfluidic paper-based device for determination of iron(II) and iron(III), Microchem. J. 188 (2023), https://doi.org/10.1016/j.microc.2023.108462.
[37] M.G. Pereira, A. Machado, A. Leite, M. Rangel, A. Bordalo, A.O.S.S. Rangel, R.B. R. Mesquita, Microfluidic paper-based device incorporated with silica nanoparticles for iodide quantification in marine source dietary supplements, Sensors 24 (2024), https://doi.org/10.3390/s24031024.
[38] N. Uhlikova, M.I.G.S. Almeida, I. McKelvie, R. Morrison, S.D. Kolev, Use of scanners for colorimetric analysis of microfluidic paper-based analytical devices (μPADs): a practical guide, Microchem. J. 191 (2023), https://doi.org/10.1016/j.microc.2023.108879.
[39] V. Vaishampayan, O. Robita Chanu, B. Sivasamy, M. Ponnuchamy, V. Karthik, A. Pendharkar, L. Srinivas Thotakura, A. Prabhu, V. Dhananjeyan, A. Kapoor, Microfluidic paper-based device coupled with 3D printed imaging box for colorimetric detection in resource-limited settings, HardwareX 15 (2023), https://doi.org/10.1016/j.ohx.2023.e00456.
[40] G. Chen, H.H. Chai, L. Yu, C. Fang, Smartphone supported backlight illumination and image acquisition for microfluidic-based point-of-care testing, Biomed. Opt. Express 9 (2018) 4604, https://doi.org/10.1364/boe.9.004604.
[41] F.T.S.M. Ferreira, R.B.R. Mesquita, A.O.S.S. Rangel, Novel microfluidic paper-based analytical devices (μPADs) for the determination of nitrate and nitrite in human saliva, Talanta 219 (2020), https://doi.org/10.1016/j.talanta.2020.121183.
[42] S.C. Kim, U.M. Jalal, S.B. Im, S. Ko, J.S. Shim, A smartphone-based optical platform for colorimetric analysis of microfluidic device, Sens Actuat. B Chem. 239 (2017) 52–59, https://doi.org/10.1016/j.snb.2016.07.159.